Korean J. Chem. Eng., **27**(6), 1738-1743 (2010)
DOI: 10.1007/s11814-010-0287-3

IR study on the reduction of NO and NO_2 by hydrazine monohydrate over Fe-BEA zeolite

Se Min Park*, Gon Seo*,†, Young San Yoo, and Hyun-Sik Han****

*School of Applied Chemical Engineering and the Center for Functional Nano Fine Chemicals,
Chonnam National University, Gwangju 500-757, Korea
**Heesung Catalyst Corporation, 1251-6 Jungwang-dong, Shihung, Gyeonggi 429-450, Korea

(*Received 2 February 2010 • accepted 4 March 2010*)

Abstract−The adsorption of NO and NO_2 and their subsequent reduction by hydrazine monohydrate (HDM) over Fe-BEA zeolite were investigated using an FT-IR spectrophotometer equipped with an *in-situ* cell. Although NO and NO_2 molecules were adsorbed on Fe species in an unaltered state, some of them reacted with oxygen atoms, resulting in the adsorption of NO_2 and NO_3^-, respectively. The reducing species that had originated from HDM on Fe-BEA selectively reduced these molecules to N_2, while a small amount of N_2O was formed in the reduction of NO by HDM. NO and NO_2 were rapidly reduced by HDM through their adsorbed state even at 150 °C, and Fe species were required for their adsorption and for the formation of reducing species from HDM.

Key words: Hydrazine Monohydrate, Fe-BEA Zeolite, NO_x

INTRODUCTION

With the expanded application of diesel engines to small passenger cars, as well as large trucks and buses, due to their high fuel efficiency, the increasing emission of nitrogen oxides (NO_x) and particulate matter, which are the most serious diesel pollutants, is causing severe air pollution. The excessive oxygen content of the diesel engine exhaust hinders the catalytic reduction of NO_x with carbon monoxide and unburned hydrocarbons (HCs) also being contained in the exhaust, compared to gasoline engines in which these pollutants can be successfully removed through balanced oxidation-reduction reactions over three-way catalysts. Even though improvements to the mechanical structure and performance of diesel engines have reduced the NO_x emissions, post treatments of their exhaust are inevitably required to meet the strict regulation for NO_x emission [1].

The selective catalytic reduction (SCR) of NO_x by urea is a promising technique for effective NO_x removal in diesel engine exhaust [1-5]. Urea-SCR deNO_x systems have already been introduced for large buses because their stable operation ensures high performance in NO_x removal [5]. However, urea-SCR suffers several disadvantages that hinder its wide application. The first issue is the inability of urea-SCR to work at low temperatures of around 150 °C, while the advancement of diesel engines has lowered their exhaust temperature to improve fuel efficiency. The second issue is ammonia slip that is emitted as a secondary pollutant when there is any change in driving condition, even though ammonia is a useful reductant for NO_x. The necessary large tanks and the complicated injection system of diluted urea solution considerably increase the operation cost of urea-SCR, especially in small passenger cars.

Nitrogen-containing materials such as ammonia and urea reduce NO_x over various catalysts, but the reaction paths among NO_x and reducing species on catalysts vary considerably because their adsorbed species are essentially different according to catalyst types. On the mixed catalysts such as Fe-Mn and Mn-Ce, the removal of lattice oxygen atoms by the reducing species initiates the reduction, producing vacant lattice oxygen site [6,7]. The adsorption and activation of NO_x on the vacant lattice oxygen sites complete the SCR cycle. However, the reaction of NO_x with reducing species on zeolite catalysts containing transition metals is more complex because various adsorbed species can be formed from NO_x and reductants on metal atoms, acid sites and metal oxide clusters contained in zeolites.

Hydrazine monohydrate (HDM) has a reducing activity as high as that of hydrazine, but it is not an explosive. Therefore, it can be stored and delivered using simple steel cans, unlike hydrazine. It is widely used as a reducing reagent for dissolved oxygen in water [8]. Since hydrazine dissociates to NH, NH_2 and NH_3 on transition metal atoms, HDM can reduce NO_x. Furthermore, the formation of hydrazinium ions on acid catalysts preserves excessively dosed HDM at the reaction with NO_x, thereby minimizing the emission of secondary pollutants [9].

Zeolites containing transition metals have been suggested as active SCR catalysts. Cu-MFI zeolite is a well-known NH_3-SCR catalyst [1,3,4], and Fe-MFI zeolites show high activities in the urea-SCR of NO_x [5,10] and in the HC-SCR of N_2O [11]. Since the large micropores of BEA zeolite, composed of a 12-membered ring (MR), are more suitable for the rapid diffusion of reactants and products than MFI zeolite composed of 10-MR, BEA zeolite containing iron species is preferred as a catalyst for industrial applications [12]. However, the verification of the catalytic role of transition metals is very different, because zeolites can contain transition metal atoms with various states such as atoms substituted in the framework, ions exchanged, metal clusters located in micropores and large agglomerates of metal oxide dispersed on the external surface. The active species of iron also varies according to the type of reaction: the iso-

---

†To whom correspondence should be addressed.
E-mail: gseo@chonnam.ac.kr

lated iron species, Fe^{3+}, is responsible for HC-SCR [11], while the very small iron oxide cluster composed of Fe^{2+}/Fe^{3+} species has high activity for the decomposition of N_2O [13].

In this study, we examine the adsorption and reaction of NO, NO_2 and HDM on an iron-substituted BEA zeolite (Fe-BEA) using a Fourier-transformed infrared (FT-IR) spectrophotometer to identify the species originating from these materials and to verify the role of iron species at the reduction that occurs among them. The IR investigation provides some understanding of the adsorbed states of NO and NO_2 on Fe-BEA and their reduction by the reducing species originating from HDM. The role of Fe species in the adsorption of NO, NO_2 and HDM and the reduction is also discussed.

EXPERIMENTAL

1. Catalyst

A Fe-BEA zeolite with a Si/Al molar ratio of 43 and BET surface area of 584 $m^2 \cdot g^{-1}$, provided by Heesung Catalyst Corp., was used as a catalyst for the reduction of NO_x by HDM. The iron content was 1.2 wt% and most of the iron atoms were substituted to the framework [13]. An H-BEA zeolite, provided by Heesung Catalyst Corp., with a Si/Al molar ratio of 52 and BET surface area of 599 $m^2 \cdot g^{-1}$ was used as the reference catalyst.

2. *In-situ* FT-IR Study on the Adsorption and Reduction of NO_x

The adsorption of NO, NO_2, and HDM and the reactions among the adsorbed species on the Fe-BEA zeolite were monitored by using an FT-IR spectrophotometer (BIO-RAD, 175C) at 150 °C [6]. A wafer of the Fe-BEA zeolite (10 mg) was charged in an *in-situ* IR cell (Graseby Specac) and evacuated at 500 °C for 1 h. The IR spectra of the adsorbed species presented on the zeolite were recorded by accumulating 16 scans at the range of 4,000-700 cm^{-1} with a resolution of 4 cm^{-1} to lower the signal-to-noise ratio.

For the reductive removal of NO and NO_2 by HDM pulses, the evacuated wafer was exposed to NO/O_2 (Hankook Special Gas, NO 450 ppmv/O_2 10%/N_2 balance) and NO_2/O_2 (Hankook Special Gas, NO_2 324 ppmv/O_2 5%/N_2 balance) mixed gas flows of 100 ml/min until an adsorption equilibrium was achieved. An HDM (64.5%, Aldrich) pulse of 0.020 mmol was injected into the flows and the IR spectra were recorded to monitor the reduction of NO and NO_2.

The consumption of HDM stored on the Fe-BEA zeolite by NO and NO_2 was also examined. An HDM pulse of 0.020 mmol was injected into the activated Fe-BEA zeolite wafer in the nitrogen flow. After 30 min, the nitrogen flow was replaced by a mixed gas flow consisting of either NO/O_2 or NO_2/O_2. The IR spectra were recorded to trace the reactions among the species adsorbed on the zeolite.

RESULTS AND DISCUSSION

1. The Adsorption of NO and NO_2

The NO_x states adsorbed on Fe-BEA vary according to their species. Fig. 1 shows the IR spectra of NO adsorbed on Fe-BEA in the presence of O_2. Following exposure to NO/O_2 mixed gas, Fe-BEA exhibited an absorption band at 1,634 cm^{-1}, accompanied by a small band at 1,870 cm^{-1}. The latter band increased rapidly, while the former band slightly decreased after 1 min and steadily maintained its height. After 10 min, a very weak shoulder band appeared at 1,578 cm^{-1}. The bands at 1,634 cm^{-1} and 1,578 cm^{-1} were attributed to NO_2 and NO_3^- adsorbed on Fe species, respectively [14-18,22-24]. The band at 1,870 cm^{-1} was considered to be related to Fe^{2+}(NO) [14-16,19-22]. Therefore, the rapid increase of the band at 1,634 cm^{-1} with the exposure of Fe-BEA to the NO/O_2 mixed gas indicated the oxidation adsorption of NO as $Fe^{n+}(NO_2)$ [23]. Since activated Fe-BEA zeolite usually have both Fe^{2+} and Fe^{3+} species simultaneously, the observed band at 1,634 cm^{-1} is attributed to NO_2 on Fe species of +2 and +3 oxidation states [13,24]. Subsequently, NO adsorbed on Fe^{2+} species to produce Fe^{2+}(NO) adsorbed species. No continuous increase in the band at 1,634 cm^{-1} with time suggested the limitation of Fe species to oxidize NO to NO_2.

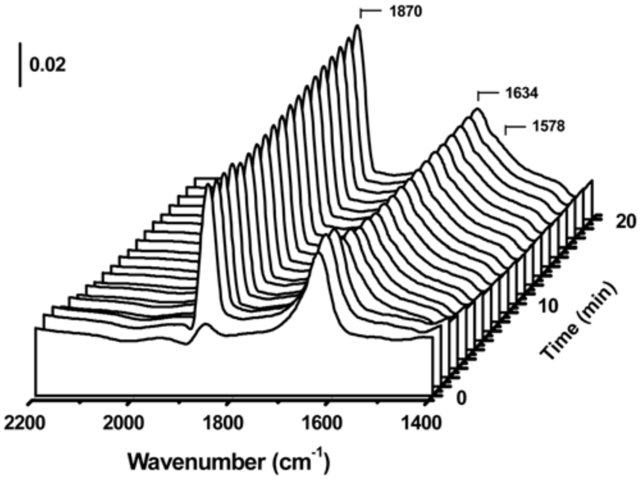

Fig. 1. IR spectra of NO adsorbed on Fe-BEA zeolite at 150 °C. Feed gas: NO 450 ppm/O_2 10%/N_2 balance, flow rate: 100 ml/min.

Compared to those of NO, the adsorbed states of NO_2 on Fe-BEA were relatively simple, as shown in Fig. 2. The gradual increases of the band at 1,634 cm^{-1} indicated that most of the NO_2 was directly adsorbed on Fe species. The initial appearance of a small band at

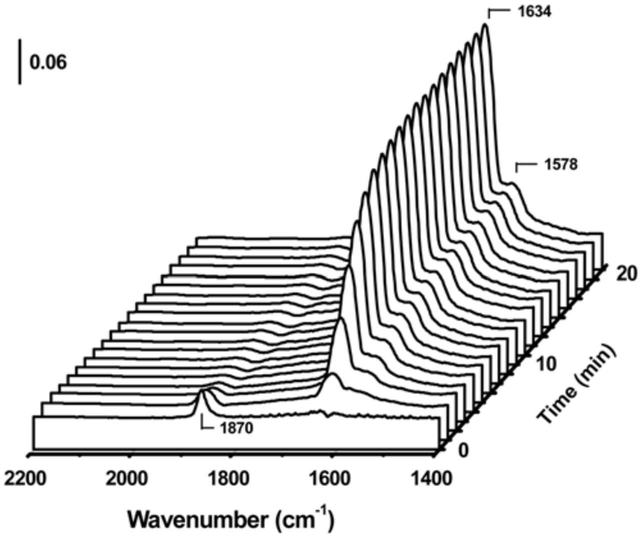

Fig. 2. IR spectra of NO_2 adsorbed on Fe-BEA zeolite at 150 °C. Feed gas: NO_2 324 ppm/O_2 5%/N_2 balance, flow rate: 100 ml/min.

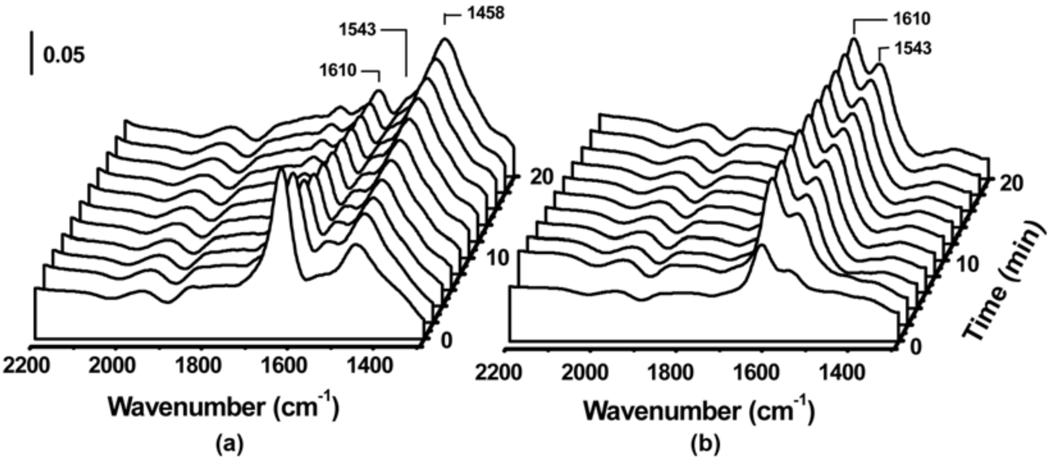

Fig. 3. IR spectra of HDM adsorbed on Fe-BEA (a) and H-BEA (b) zeolites at 150 °C. Pulse size of injected HDM: 0.02 mmol.

1,870 cm^{-1}, which subsequently disappeared, was due to the formation of Fe^{2+}(NO) on Fe-BEA as the adsorbed NO_2 lost one oxygen atom. A small band at 1,578 cm^{-1} revealed the adsorption of NO_2 as NO_3^- by combining with oxygen atom.

The absence of any adsorption bands at the exposure of the NO/O_2 and NO_2/O_2 mixed gases on H-BEA confirmed the adsorption of NO and NO_2 on Fe species, not on acid sites. However, the immediate disappearance of the bands related to NO and NO_2 adsorbed on Fe-BEA following evacuation indicated the weak adsorptions of these gaseous molecules. On the contrary, the NO_3^- species adsorbed on Fe-BEA were retained under evacuation because of its strong adsorption.

HDM greatly affected the IR spectra upon its adsorption on Fe-BEA and H-BEA, as shown in Fig. 3. The addition of an HDM pulse to activated Fe-BEA induced the appearance of an intense band at 1,627 cm^{-1}, accompanied by a small band at 1,458 cm^{-1}. After 6 min, the former disappeared and the latter gradually increased. The bands at 1,610 cm^{-1} and 1,543 cm^{-1} were steadily observed after 10 min. The band at 1,627 cm^{-1} was attributed to water adsorbed on zeolites and that at 1,458 cm^{-1} to ammonium ion adsorbed on Fe species [14,17-19,25]. The hydrazinium ions formed on acid sites caused the bands at 1,610 and 1,543 cm^{-1} [26-28]. Therefore, the spectra indicated the presence of both hydrazinium and ammonium ions on the Fe-BEA upon the adsorption of HDM. The water contained in HDM was responsible for the band initially observed at 1,627 cm^{-1}. However, the adsorption bands of hydrazinium and ammonium ions were retained due to their strong adsorption, while water was removed by desorbing into the flow. The addition of an HDM pulse to H-BEA induced the appearance only of those bands related to the formation of hydrazinium ions on the acid sites. The persistent presence of the bands indicated the conversion of hydrazinium ions to ammonium ions on the Fe species. Since the absorption bands attributed to NH_x adsorbed on Fe species, including NH, NH_2 and NH_3, were observed at similar wavenumbers to that of the ammonium ions, the chemical nature of the adsorbed species originating from HDM could not be definitely verified by the IR spectra alone [17-19]. Therefore, the ammonium ions adsorbed on Fe-BEA were denoted as the mixture of all NH_x species, including their cations, in this paper.

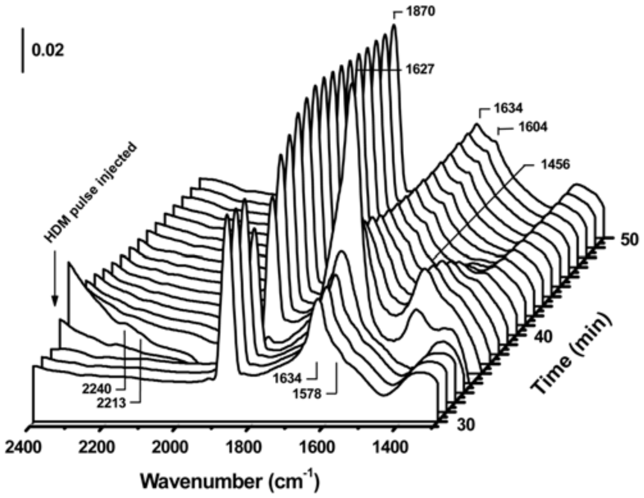

Fig. 4. Removal of NO by an HDM pulse over Fe-BEA zeolite at 150 °C. Reaction conditions: feed gas; NO 450 ppmv/O_2 10%/N_2 balance, flow rate; 100 ml/min, pulse size of injected HDM; 0.02 mmol.

2. The Reaction between HDM and NO_x over Fe-BEA

The reduction of NO and NO_2 by HDM over Fe-BEA can be effectively monitored using an *in-situ* IR spectrophotometer. Fig. 4 shows the IR spectra recorded in the reduction of adsorbed NO by HDM. The appearance of three bands at 1,870, 1,634 and 1,578 cm^{-1} indicated the presence of NO, NO_2 and NO_3^- species adsorbed on Fe-BEA, respectively, as discussed above. The addition of HDM significantly reduced the band at 1,870 cm^{-1} but considerably increased the band at 1,627 cm^{-1}, which was assigned to water adsorbed on the zeolite. The appearance of small bands at 2,240 and 2,213 cm^{-1}, attributed to N_2O adsorbed on Fe species, confirmed the formation of N_2O in the reduction of NO by HDM [29,30-32]. The band at 1,456 cm^{-1}, attributed to ammonium ions, increased after the injection of the HDM pulse, but decreased with the consumption of HDM. The consumption of HDM gradually restored the initial IR spectrum obtained after the exposure of Fe-BEA to the NO/O_2 mixed gas flow. However, the retention of a new band at

1,604, attributed to $NO_2(NH_4^+)_y$, indicated the retention of a reaction intermediate formed during the reduction [14]. After the recovery of the initial spectrum, a pulse of HDM was injected again to confirm the catalytic reduction of NO by HDM on Fe-BEA. Following the injection of the second HDM pulse, the appearance of spectra identical to those of the first HDM pulse clearly demonstrated that NO was effectively reduced by HDM over Fe-BEA.

NO can be reduced by HDM to N_2 and H_2O via various reaction pathways. The most well-known intermediate for the reduction is $NO_2(NH_4^+)_y$, which is formed by the reaction between ammonium ions originating from HDM and NO_2 oxidized from NO on Fe species [14]. Although the oxidation of NO to NO_2 over Fe-BEA was suggested as the rate-determining step for the reduction of NO by ammonia [10,24], the IR spectra could not provide a direct evidence for the NO reduction via NO_2 because the overall reduction of NO reflected on them. Since N_2O was formed by the reaction between NO and NH, the appearance of bands related to N_2O also confirmed the formation of NH species from HDM via heterogeneous dissociation, even though the very small size of these bands indicated the rareness of the NH formation [28,30]. The possible reactions derived from the IR spectra are listed below:

$$N_2H_4 \rightarrow 2NH_2 \rightarrow NH_3 + NH \tag{1}$$

$$NH_2 + NO \rightarrow N_2 + H_2O \tag{2}$$

$$NH + NO \rightarrow N_2O + H^+ + e \tag{3}$$

$$NH_3 + H^+ \rightarrow NH_4^+ \tag{4}$$

$$NO + 1/2O_2 \rightarrow NO_2 \tag{5}$$

$$2NH_4^+ + NO_2 + NO \rightarrow NO_2(NH_4^+)_2 + NO \rightarrow 2N_2 + 3H_2O + 2H^+ \tag{6}$$

The reduction of NO_2 by HDM over Fe-BEA was very simple, as shown in Fig. 5. As aforementioned, the two bands that appeared at 1,634 and 1,578 cm^{-1} following the exposure of Fe-BEA to NO_2/O_2 mixed gas were attributed to NO_2 and NO_3^- adsorbed on Fe species, respectively. The removal of these bands upon injection of the HDM pulse and their subsequent restoration upon the HDM consumption indicated the effective reduction of NO_2 by HDM. The small bands at 1,869 and 1,627 cm^{-1} that were tentatively observed during this reduction were attributed to NO adsorbed on Fe^{2+} species and water adsorbed on zeolite, respectively. The appearance of the NO band reflected the step-wise removal of an oxygen atom from NO_2. The band related to water was attributed to the water contained in HDM itself or produced in the reduction. The absence of any absorption bands attributable to N_2O around 2,200 cm^{-1} indicated the highly selective reduction of NO_2 to N_2 by HDM.

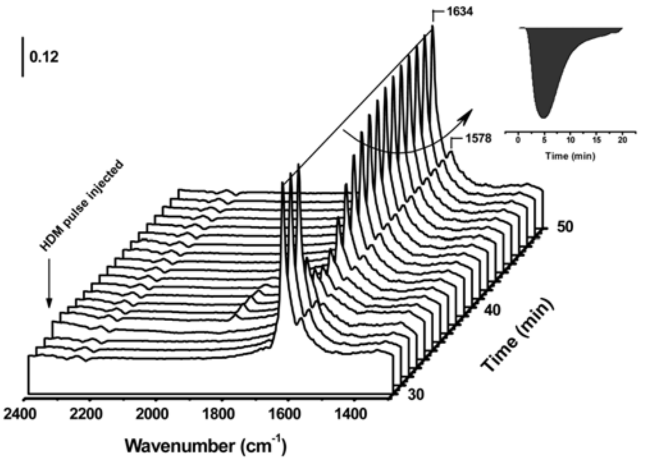

Fig. 5. Removal of NO_2 by an HDM pulse over Fe-BEA zeolite at 150 °C. Reaction conditions: feed gas; NO_2 324 ppmv/O_2 5%/N_2 balance, flow rate; 100 ml/min, pulse size of injected HDM; 0.02 mmol.

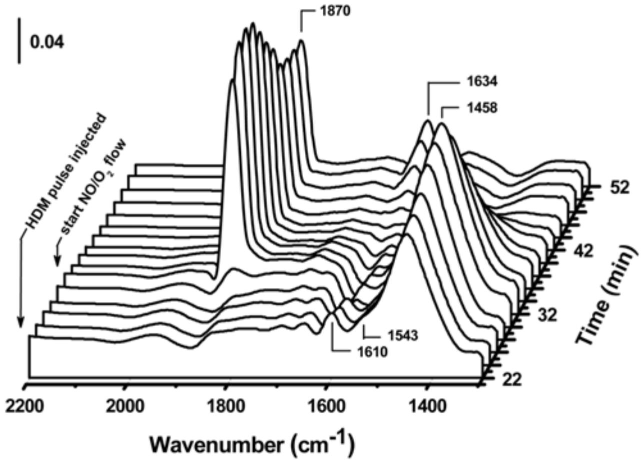

Fig. 6. Reduction of NO by HDM adsorbed over Fe-BEA zeolite at 150 °C. Reaction conditions: feed gas; NO 500 ppmv/O_2 5%/N_2 balance, flow rate; 100 ml/min, pulse size of injected HDM; 0.02 mmol.

Fig. 6 shows the IR spectra of the species formed on Fe-BEA due to the adsorption of HDM and their consumption by the NO/O_2 mixed gas flow. The injection of an HDM pulse induced two bands at 1,610 and 1,543 cm^{-1}, attributed to hydrazinium ions, and one band at 1,458 cm^{-1}, attributed to ammonium ions, as aforementioned. Most of the former were converted to the latter after about 20 min. The supply of the NO/O_2 mixed gas flow drastically decreased the bands related to hydrazinium and ammonium ions, while the increase of the band at 1,870 cm^{-1}, related to Fe^{2+}(NO), was considerably small. These results indicated that the hydrazinium and ammonium ions adsorbed on Fe-BEA were rapidly consumed in the reduction of NO. Although whether the reduction paths of NO were either a direct reduction or via oxidative adsorption state NO_2 was not clarified. The absence of the band at 1,634 cm^{-1} might reflect the easy reduction of NO_2 compared to NO over Fe species. After the consumption of HDM, the increase in the band at 1,870 cm^{-1} indicated the formation of Fe^{2+}(NO). However, the band at 1,634 cm^{-1} was gradually increased until 60 min due to the formation of Fe^{3+} species with releasable oxygen atoms sites and subsequent delivery of one oxygen atom to an NO molecule leading to its conversion to the NO_2. The accompanying decrease of the band at 1,870 cm^{-1} also confirmed the gradual conversion of NO to NO_2.

The reduction of NO_2 by the HDM-originated species that was adsorbed on Fe-BEA exhibited more complex IR spectra, as shown in Fig. 7. The injected HDM pulse produced hydrazinium and ammonium ions on Fe-BEA. The supply of the NO_2/O_2 mixed gas flow simultaneously increased both the bands related to water and ammonium ions while decreasing the bands related to hydrazinium

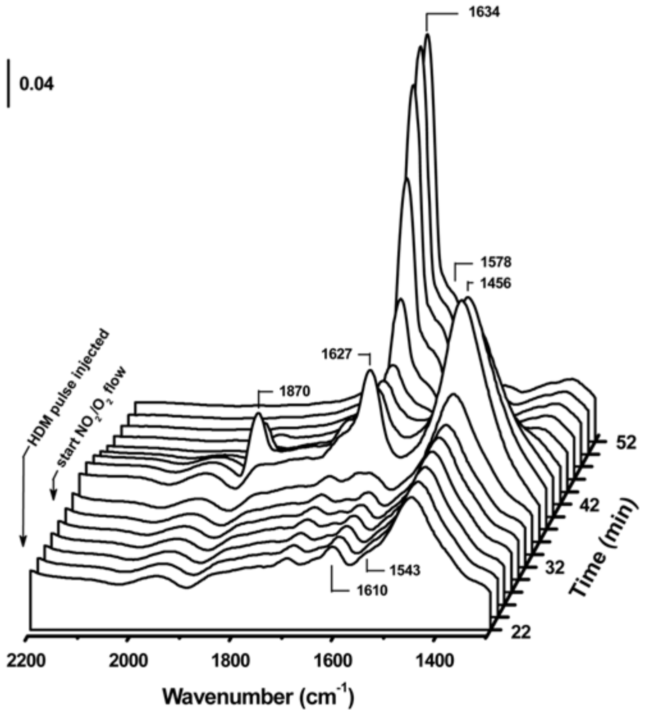

Fig. 7. Reduction of NO_2 by HDM adsorbed over Fe-BEA zeolite at 150 °C. Reaction conditions: feed gas; NO_2 324 ppmv/O_2 5%/N_2 balance, flow rate; 100 ml/min, pulse size of injected HDM; 0.02 mmol.

ions. Since the band assigned to ammonium ions also reflected the reducing species such as NH, NH_2 and NH_3, the further increase of this band suggested that NO_2 accelerated the dissociation of hydrazinium ions to various reducing species over Fe-BEA. The sharp increase of the band related to water indicated the rapid reduction of NO_2 by the reducing species present on Fe-BEA. The tentative observation of the 1,870 cm^{-1} band confirmed the formation of NO from the reduction of NO_2, suggesting the step-wise reduction. After the adsorbed hydrazinium and ammonium ions were consumed, the original IR spectrum of Fe-BEA exposed to the NO_2/O_2 mixed gas flow was restored (Fig. 2).

An IR study of the adsorption of NO on Fe-BEA indicates the temporal change in the adsorbed state of NO: NO was initially adsorbed as NO_2, but later Fe^{2+}(NO) species became more predominant. The adsorption of NO as NO_3^- was very small. This observation suggests the strong adsorption of NO on Fe species sites with an oxygen atom that can be easily released, thereby producing the Fe^{n+}(NO_2) state. After all these Fe species had been consumed by the NO adsorption, NO was adsorbed on the Fe^{2+} species as Fe^{2+}(NO). Compared to that of NO, the adsorption of NO_2 on Fe-BEA was very simple. Most of the NO_2 was principally adsorbed on Fe species, although the dissociation of oxygen atoms from NO_2 caused the initial adsorption of NO on Fe species.

HDM has various adsorbed states such as hydrazinium and ammonium ions. The adsorption of HDM on the Brønsted acid sites of H-BEA induces intense bands only related to hydrazinium ions. However, on Fe-BEA, HDM was adsorbed not only as hydrazinium ions, but also as ammonium ions. The gradual increase of the band related to ammonium ions in conjunction with the decrease of the band related to hydrazinium ions strongly suggests the conversion of hydrazinium ions to ammonium ions on Fe species. When the amount of NO_x adsorbed on Fe-BEA is smaller than that of the supplied HDM, some of the HDM is not consumed in the reduction. However, the storage of HDM as ammonium ions (Fig. 4) minimized the exhaust of the secondary pollutants.

HDM reacted with the NO and NO_2 adsorbed on Fe-BEA and mainly produced water as the product of the selective reduction. Although the formation of N_2O was detected in the reduction of NO by HDM, its absorption bands were extremely small and disappeared quickly, indicating HDM's high selectivity for the reduction of NO and NO_2 to N_2. In a subsequent paper, we will present our further study on the catalytic reduction of NO_x by HDM in a continuous flow reactor.

CONCLUSIONS

NO and NO_2 were adsorbed on the Fe species of Fe-BEA in various states. Oxygen atoms were also involved in this adsorption for the oxidation of NO and NO_2. Fe species catalyzed the dissociation of HDM to ammonium ions, including NH_x species, as indicated by the appearance of the band related to ammonium ions only on Fe-BEA and not on H-BEA. Dissociated reducing species originating from HDM rapidly reduced the adsorbed species of NO and NO_2, even at 150 °C. Although a small amount of N_2O was formed in the reduction of NO with HDM, the selectivity for the reduction to N_2 was generally high.

ACKNOWLEDGEMENTS

This work was a part of the project 'New deNO_x system for purification in diesel engine exhaust' and one of the authors (G. Seo) is grateful for the financial support of Heesung Catalyst Corporation.

REFERENCES

1. Z. Liu and S. I. Woo, *Catal. Rev.*, **48**, 43 (2006).
2. F. Klingstedt, K. Arve, K. Eränen and D. Y. Murzinn, *Acc. Chem. Res.*, **39**, 273 (2006).
3. J. H. Baik, S. D. Yim, I.-S. Nam, Y. S. Mok, J.-H. Lee, B. K. Cho and S. H. Oh, *Ind. Eng. Chem. Res.*, **45**, 5258 (2006).
4. O. Kröcher and M. Elsener, *Ind. Eng. Chem. Res.*, **47**, 8588 (2008).
5. J. Kusaka, M. Sueoka, K. Takada, Y. Ohga, T. Nagasaki and Y. Daisho, *Int. J. Eng. Res.*, **6**, 11 (2005).
6. S. M. Park, J. W. Park, H.-P. Ha, H.-S. Han and G. Seo, *J. Mol. Catal. A: Chem.*, **273**, 64 (2007).
7. L. Cao, L. Ratts, A. Yezerets, N. W. Currier, J. M. Caruthers, F. H. Ribeiro and W. N. Delgass, *Ind. Eng. Chem. Res.*, **47**, 9006 (2008).
8. J.-S. Moon, K.-K. Park, J.-H. Kim and G. Seo, *Appl. Catal. A: Gen.*, **184**, 41 (1999).
9. K. Hadjiivanov, D. Klissurski, G. Ramis and G. Busca, *Appl. Catal. B: Environ.*, **7**, 251 (1996).
10. M. Devadas, O. Kröcher, M. Elsener, A. Wokaun, G. Mitrikas, N. Söger, M. Pfeifer, Y. Demel and L. Mussmann, *Catal. Today*, **119**, 137 (2007).
11. M. Schwidder, M. S. Kumar, K. Klementiev, M. M. Pohl, A. Brückner and W. Grünert, *J. Catal.*, **231**, 314 (2005).

12. T. Tabata, H. Ohtsuka, L. M. F. Sabatino and G. Bellussi, *Micropor. Mesopor. Mater.*, **21**, 517 (1998).
13. M.-Y. Kim, K. W. Lee, J.-H. Park, C.-H. Shin, J. Y. Lee and G. Seo, *Korean J. Chem. Eng.*, **27**, 76 (2010).
14. G. Mul, J. Perez-Ramirez, F. Kapteijn and J. A. Moulijn, *Catal. Lett.*, **80**, 129 (2002).
15. H.-Y. Chen, X. Wang and W. M. H. Sachtler, *Appl. Catal. A: Gen.*, **194**, 159 (2000).
16. G. Qi and R. T. Yang, *Appl. Catal. B: Environ.*, **60**, 13 (2005).
17. R. Brosius, P. Bazin, F. Thibault-Starzyk and J. A. Martens, *J. Catal.*, **234**, 191 (2005).
18. G. Qi, J. E. Gatt and R. T. Yang, *J. Catal.*, **226**, 120 (2005).
19. L. J. Lobree, I.-C. Hwang, J. A. Reimer and A. T. Bell, *J. Catal.*, **186**, 242 (1999).
20. R. Joyner and M. Stockenhuber, *J. Phys. Chem. B*, **103**, 5963 (1999).
21. I. Yuranov, D. A. Bulushev, A. Renken and L. Kiwi-Minsker, *Appl. Catal. A: Gen.*, **319**, 128 (2007).
22. R. Q. Long and R. T. Yang, *J. Catal.*, **207**, 224 (2002).
23. L. J. Lobree, I.-C. Hwang, J. A. Raeimer and A. T. Bell, *Catal. Lett.*, **63**, 233 (1999).
24. R. Q. Long and R. T. Yang, *J. Catal.*, **207**, 274 (2002).
25. J. M. G. Amores, V. S. Escribano, G. Ramis and G. Busca, *Appl. Catal. B: Environ.*, **13**, 45 (1997).
26. M. A. Larrubia, G. Ramis and G. Busca, *Appl. Catal. B: Environ.*, **30**, 101 (2001).
27. G. Ramis and M. A. Larrubia, *J. Mol. Catal. A: Chem.*, **215**, 161 (2004).
28. B. R. Wood, J. A. Reimer, A. T. Bell, M. T. Janicke and K. C. Ott, *J. Catal.*, **225**, 300 (2004).
29. A. Waclaw, K. Nowinska, W. Schwieger and A. Zielinska, *Catal. Today*, **90**, 21 (2004).
30. G. Ramis, L. Yi, G. Busca, M. Turco, E. Kotur and R. J. Willey, *J. Catal.*, **157**, 523 (1995).
31. B. R. Wood, J. A. Reimer and A. T. Bell, *J. Catal.*, **209**, 151 (2002).
32. L. A. Isupova, A. A. Budneva, E. A. Paukshits and V. A. Sadykov, *J. Mol. Catal. A: Chem.*, **158**, 275 (2000).